SMARTCELLS™ – ENABLING FAST AND ACCURATE ELECTRONICS THERMAL DESIGN

MENTOR GRAPHICS, MECHANICAL ANALYSIS DIVISION

WHITEPAPER

MECHANICAL ANALYSIS

www.mentor.com

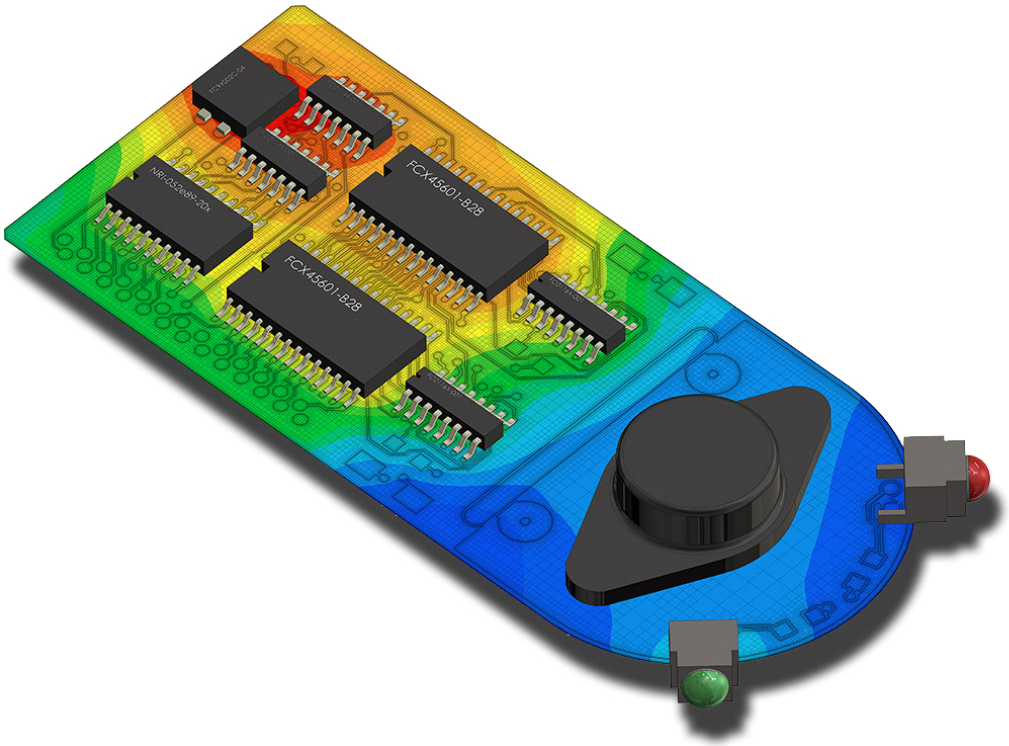

This white paper introduces the concept of SmartCells™ in the context of Computational Fluid Dynamics (CFD) simulation software. They exist in FloTHERM XT™, a CAD enabled electronics cooling simulation tool supplied by Mentor Graphics (Ref 1). This document will explain what they are, how they differ from other meshing approaches employed in the CFD industry, and their benefits to CFD users and electronics thermal designers.

SmartCells:

- Attain high levels of simulation accuracy for mesh counts, typically 10 times less than traditional CFD meshes, by using Cartesian based meshes.
- Increase productivity by employing numerical approaches and engineering models embedded within FloTHERM XT which reduces, generally by an order of magnitude, the manual time spent by traditional CFD tool users in meshing their geometries.
- Allow for automated mesh generation because of their built-in artificial intelligence, based on decades of industrial CFD simulation experience using engineering model data.
- Provide turbulent boundary layer simulation accuracy in all fluid flow processes while handling complex geometries which may have many fluid-solid control volume zones in one mesh SmartCell.
- Lead to thermal design workflow gains of typically x2 to x10 fold through the associated built-in pre-processing and user experience benefits inside FloTHERM XT.

INTRODUCTION

Computational Fluid Dynamics is a well-established computer-aided engineering simulation software industry of over 40 years standing with the commercial sector accounting for over $1Bn/yr. in revenues worldwide today (Ref 2). The bulk of CFD simulation (over 90%) carried out globally is based on the finite volume (FV) methodology using a Reynolds-averaged Navier-Stokes (RANS) approach because of its robust nature and computational efficiency (Ref 2). CFD is based on well-accepted numerical methods for solving the fundamental Navier-Stokes equations that govern fluid flow, heat and mass transfer (Ref 3). But the technology enablers for the traditional CFD industry invariably are a synergy between numerical and engineering techniques and analytical methods that are 30 – 40 years old (Ref 4). Indeed, the vast majority of CFD carried out in the world today is based on variants of the tried-and-proven k-ε turbulence model, the accepted workhorse of the industry that is now over 40 years old (Ref 5).

Users of traditional CFD simulation tools for the first time can find them very difficult to use because the user has to master very complicated pre-processing (geometry and grid generation) approaches and frequently the codes themselves demand of users a deep understanding of the physics and numerical algorithms underlying them because of their inherent mathematical nature. And invariably the quality of a CFD prediction is very much affected by the pre-processing approach employed. By applying new and more modern analytical methods to numerical CFD tasks to resolve phenomena describing fluid flow, heat and mass transfer the required user skills for high accuracy near-wall mesh building and the manual time spent on this task can be reduced. The use of SmartCells in CFD simulations will lead to a coarser mesh being applied to a given application to capture the physical phenomena being resolved (e.g. turbulence vortices, thin channels etc.) due to the implementation of more modern engineering data approaches (Ref 1). As a result, the SmartCell approach enables a reduced cell count for a CFD simulation compared to traditional CFD mesh approaches that are based on a fine resolution of boundary layers. Instead, it enables the automation of the meshing process completely with very low numerical skills or time requirements for the engineer or the CFD analyst using them.

The SmartCell approach to CFD has proven successful over the last 20 years for a wide range of industrial benchmarks and applications, and is regularly employed by OEMs and Tier 1 suppliers in the electronics, automotive, aerospace and other industries. Ultimately, the benefit from these synergies of numerical and engineering techniques must be seen in comparison with traditional CFD approaches. With the speed of manufacturing design cycles ever increasing, and always in the context of ever-present Product Lifecycle Management (PLM) software that all engineers use in order to improve their designs, engineers need CFD simulation results ever faster but without loss in accuracy (Ref 6).

The approach described by this white paper enables the use of CFD in design processes by non-experts and experts alike, through the automation of the pivotal meshing task without compromising the final result accuracy even with coarse meshes compared to typical CFD meshes. SmartCells are ideally suited for design processes that "frontload" CFD simulations during conceptual design through to manufacturing, improving product quality, reliability and time-to-market (Ref 8). Applicability of the SmartCell approach will be illustrated through benchmarks with a pin-fin heatsink and water-cooled cold plate.

NUMERICAL FOUNDATION OF SMARTCELLS

To understand SmartCells one must first understand the other meshing types typically used in traditional finite volume CFD simulation codes. These tend to include unstructured triangular, structured triangular, structured curvilinear, immersed boundary Cartesian meshes as well as SmartCells (see Table 1 - Ref 6). Table 1 shows a mathematical formulation of CFD simulation accuracy, $\|LTE\|_{L1}$, related to the various CFD meshing approaches used (the lower the LTE number the more accurate the CFD prediction is). The table clearly shows that to offset accuracy issues in unstructured triangular, structured triangular, and structured curvilinear meshes versus cut-cell Cartesian and SmartCell meshes, traditional CFD codes require more and more cell counts to be added to the simulation. This obviously has both a memory and a CPU overhead associated with it.

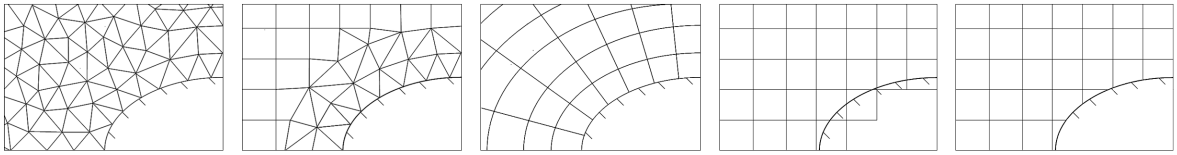

Mesh	Unstructured triangular		Structured triangular		Structured curvilinear		Cartesian [Aftosmis]		FloTHERM XT SmartCells	
	Cells	$\|\|LTE\|\|_{L1}$	Cells	$\|\|LTE\|\|_{L1}$	Cells	$\|\|LTE\|\|_{L1}$	Cells	$\|\|LTE\|\|_{L1}$	Cells	$\|\|LTE\|\|_{L1}$
Results	128	0.52552	144	0.37926	144	0.30998	138	0.03065	140	0.03014
	505	0.22529	525	0.07571	525	0.09223	507	0.00930	516	0.00916
	1918	0.11936	2001	0.01565	2001	0.02422	1928	0.00246	1944	0.00235
	7490	0.05940	7809	0.00347	7809	0.00629	7549	0.00059	7526	0.00058

Table 1: Comparing CFD mesh types with the numbers of cells required to achieve a given level of numerical solution accuracy.

It is clear from Table 1 that FloTHERM XT can generate accurate results with low Cartesian cell counts when compared to multi-millions of cells typically necessary for the same level of accuracy in traditional CFD codes. This is in part due to the numerical methods inherent in SmartCells and in part due to Cartesian cells not suffering from skewed accuracy issues typically associated with tetrahedral, hybrid and polygonal meshes used most frequently in traditional CFD approaches.

Conventional wisdom with the application of CFD is that one needs to add more and more computational grid cells in any given real-world simulation to get higher and higher accuracy by resolving finer and finer details at crucial wall boundary layers in particular. With geometrically complicated applications that include complex narrow passageways for instance, this may involve hundreds of millions of computational cells with the incumbent memory, CPU and post-processing overheads that come with these large models. And these are always necessary to get an accurate traditional CFD solution. However, this approach based on 1980s thinking is insatiable with regard to CPU demands, and invariably absorbs all the available computational resources, and more besides. Indeed, it could be argued that this bottleneck has been the single biggest barrier to the democratization of CFD usage in the last 25 years (Ref 1). This paper contends that there is another approach to industrial-level RANS CFD that is both smarter, computationally more efficient, just as effective, well validated, but uses orders of magnitude fewer cells, and therefore uses much less computational resource for the same level of accuracy as traditional CFD approaches. And it is also embedded within CAD and Product Lifecycle Management (PLM) workflows which is intuitively the most optimal place for CFD simulation to be thus enhancing user productivity in one familiar CAD/PLM interface.

In engineering design simulation practice today, whatever the industry, PLM concepts are widely deployed by engineers as the means by which 3D manufactured product data are used and maintained consistently during an entire product's lifecycle and across all its design changes (Ref 1). The basis of the PLM concept is the availability of complex 3D product model data within a mechanical Computer-aided Design (CAD) system as its central element. 3D product model data are therefore both the foundation and starting point for all virtual prototyping and physical engineering simulations today. The performing of fluid flow simulations using CFD in such a CAD-embedded context is obviously very attractive, as it can not only accelerate the design process, but make these processes more predictable and reliable, against a background of increasing design complexity and dependence on external development partners.

It is essential to note that all major CAD systems were created 20-30 years ago and were optimized as design tools and only later the necessity for embedding CAE (and in particular CFD) was recognized. Therefore it was logical that for some period in the 1980s and 1990s that CFD continued on an independent development trajectory. Nevertheless, from the standpoint of using CFD during engineering design, and as a requirement of all PLM roadmaps, the need to fully embed CFD within CAD becomes more and more pressing (Ref 9). The biggest obstacle to achieving this is high resource requirements for performing CFD calculations as applied to typical real world complex 3D CAD geometries. In particular, such CFD analyses based on solving the Navier-Stokes equations have specific requirements for detailed grid resolution of flows near the fluid/solid boundaries. Such obstacles first appear during the grid generation stage of CFD followed by more problems at the numerical solution stage. In addition, highly qualified CFD experts are usually required to do such traditional simulations but such skillsets are rarely available in design engineers. In order to resolve this issue and make CFD calculations less resource consuming and available for design engineers, the "Engineering Fluid Dynamics" (EFD) approach (Ref 1) was developed in the 1990s and this has extended into the product FloTHERM XT by Mentor Graphics Corporation today. This CFD approach inside FloTHERM XT is based on 2 main principles:

- Direct use of native CAD as the source of geometry information;
- Synergy of full 3D CFD modeling with simpler engineering methods in the cases where grid resolution is insufficient for full 3D simulation.

THE SMARTCELL TECHNIQUE

This synergy of CAD and 3D numerical models is a critical element which allows FloTHERM XT to reduce resource requirements on grid generation and numerical solution stages by an order of magnitude compared to traditional CFD approaches. It simplifies obtaining CFD results, and enables usage of complex CAD models as a source of geometry information. Surface and volume mesh grid generators in traditional CFD tools are also usually based on body-fitted algorithms. An alternative approach is to use an immersed-body grid (Ref 6). In this approach the creation of the mesh starts independently from the geometry itself and the cells can arbitrarily intersect the boundary between a given solid and fluid (see Figure 1 of a heatsink).

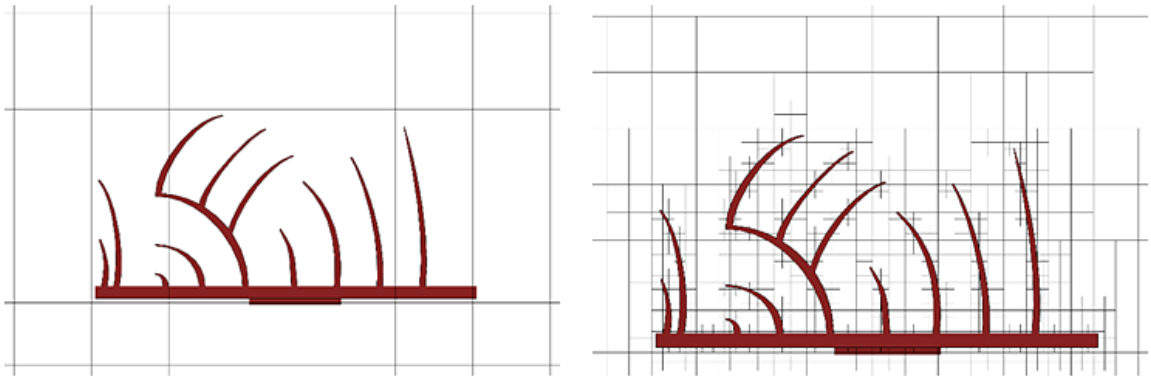

Figure 1: Cartesian immersed-body grid without grid cell refinement (left) and with grid cell refinement (right).

Such an immersed-boundary grid can be defined as a set of cuboids (rectangular cells) which are adjacent to each other and to the external boundary of the computational domain, orientated along the Cartesian coordinates. Cuboids intersected by the surface can be treated in a special way, described later in this paper, according to the boundary conditions defined on the surface. Each cuboid can be refined to 8 smaller cuboids (Figure 1) for better resolution of geometry or fluid flow singularities. It should be pointed out that the immersed body grid approach can be implemented for tetrahedral and other types of elements but in terms of numerical approximation accuracy and ease of implementation, Cartesian grids are the most preferable as they are inherently the most accurate cell type available for CFD.

As a result of using Cartesian-based grids for a given geometry, there will always be cells which are located fully in a solid body (solid cells), in fluid zones (fluid cells), and finally cells which will intersect the immersed boundary. In the simplest case, a Cartesian cell on the fluid/solid boundary consists of 2 control volumes (CV): a fluid CV and a solid CV. Within one single cell it is possible to have an arbitrary number of control volumes: 3 in case of one thin wall (fluid CV - solid CV - fluid CV) or more in case of several layers of materials with different properties inside of a thin wall (Figure 2). This underlying philosophy of accommodating multiple CVs inside one mesh cell is what we call SmartCells. It can typically handle 20 CVs inside one SmartCell.

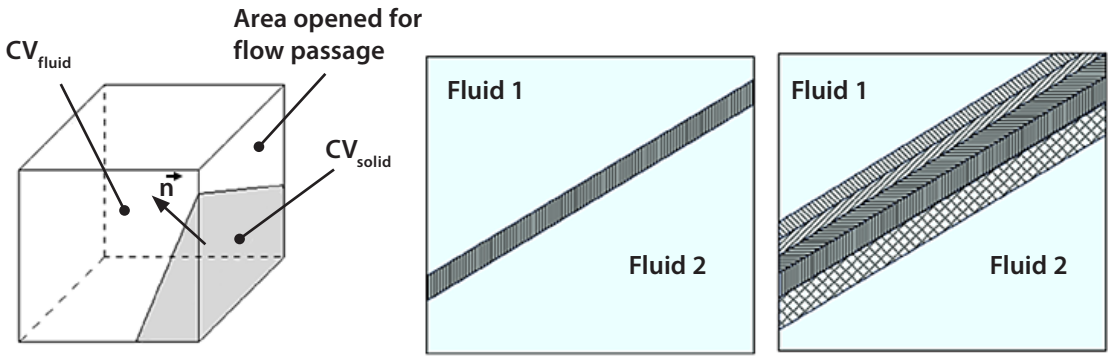

Figure 2: A "SmartCell" in the simplest case having 2 control volumes (CV) (left), with 3 control volumes (fluid-solid-fluid) in case of a thin solid wall (middle) and with 7 control volumes in the case of a thin solid wall having 5 layers with different material properties (right).

In addition to resolving two or more CVs inside one SmartCell we have devised some unique engineering techniques over the years (e.g. boundary layer treatments, thin wall treatments, thin channel treatments) that can be applied to these control volumes, in order to calculate shear stresses or heat fluxes in a correct way, if there is not enough grid resolution to resolve such phenomena by direct numerical modeling. These techniques will be described below. This approach of resolving the cells at the fluid/solid boundary we have called the "SmartCells" technique. Our unique approach involves a combination of fluid and solid control volumes inside one SmartCell, where in order to achieve industrial levels of results accuracy, engineering methods have to be applied in addition to 3D full scale numerical modeling of continuous media in both solid and fluid zones. For each control volume, all necessary geometrical parameters are calculated by extracting the corresponding data from the native CAD model. This allows us to specify all aspects of the geometry and to take the PLM data of an MCAD package into parametric CFD simulations very easily.

The FloTHERM XT SmartCells technique also includes "CAD/CFD bridge technology" which allows for good resolution of geometry features even in the case of relatively coarse meshes. Multilayer control volumes are increasingly essential for fluid flow modeling, and for heat transfer phenomena, including contact resistances and Joule heating calculations within a solid body (this being a fully-coupled multi-physics application). The solid and fluid control volumes can be alternated many times within each SmartCell (see Figure 3).

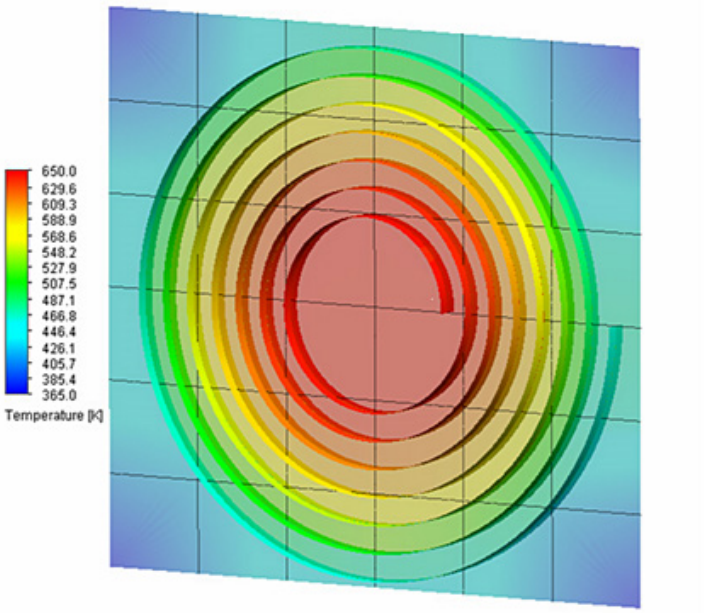

Figure 3: Multiple control volumes (solid-fluid-solid-fluid-.. etc.) for an array of SmartCells simulating a Joule Heating Coil.

SYNERGISTIC 3D MODELING & ENGINEERING TECHNIQUES IN SMARTCELLS

Within fluid regions of a SmartCell, fluid flow phenomena can be described by a system of 3-D differential equations of mass conservation of the fluid media, its momentum and energy, and turbulence characteristics. FloTHERM XT software, which is uniquely based on SmartCell techniques, is even able to consider both laminar and turbulent flows (Ref 11) in the same domain. Laminar flows occur at low values of Reynolds number. When the Reynolds number in a domain exceeds a certain critical value the flow naturally transits smoothly to turbulent flow. To simulate turbulent flows, the Favre-averaged Navier-Stokes equations are used by FloTHERM XT, where time-averaged effects of the flow turbulence on the flow parameters are considered, whereas the large-scale, time-dependent phenomena are taken into account directly. Through this procedure, extra terms known as the Reynolds stresses appear in the equations for which additional information must be provided. To close this system of equations, FloTHERM XT employs transport equations for the turbulent kinetic energy and its dissipation rate, using the modified k-ε turbulence model with damping functions proposed by Lam and Bremhorst (Ref 12).

Within solid regions of a SmartCell, FloTHERM XT calculates two kinds of physical phenomena: heat conduction and direct electrical current, with the resulting Joule heating being a source of heat in the energy equation. Each of these phenomena is described by an appropriate 3-D differential equation in partial differences. If a solid consists of several solid materials attached to each other in one cell, then the thermal contact resistances between them can be taken into account when calculating the heat conduction. As a result, a solid temperature step appears on the contact surfaces. The energy exchange between the fluid and solid media is calculated via the heat flux in the direction normal to the solid/fluid interface taking into account the solid surface temperature and the fluid boundary layer characteristics, and radiation heat exchange if considered. As a result of radiation calculations, the appropriate heat fluxes are taken into account in SmartCells for immersed fluid-solid boundaries or in solid cells within semi-transparent solid bodies.

The biggest issue for Cartesian immersed-body grids in CFD today is the resolution of boundary layers on coarse meshes. In most practical cases, such grids can be too coarse for the accurate solution of Navier-Stokes equations especially within a high-gradient boundary layer. Therefore, in order to calculate skin friction and heat flux at the wall, the Prandtl approach for boundary layers is used (Ref 13). The key idea behind this approach is similar to the wall function approach used in traditional CFD codes.

However, the wall treatment that forms part of the FloTHERM XT SmartCells technology uses a novel and original Two-Scale Wall Function (2SWF) approach that consists of two methods for coupling the boundary layer calculation with the solution of bulk flows and an automated hybrid approach:

1. A thin boundary layer treatment that is used when the number of cells across the boundary layer is not enough for direct, or even simplified determination of the flow and thermal profiles (Figure 4);
2. A thick boundary layer approach when the number of cells across the boundary layer exceeds that requirement to accurately resolve the boundary layer (Figure 4);
3. In intermediate cases, the FloTHERM XT code automatically employs a compilation of the two above-mentioned approaches, ensuring a smooth transition between the two models (Figure 4).

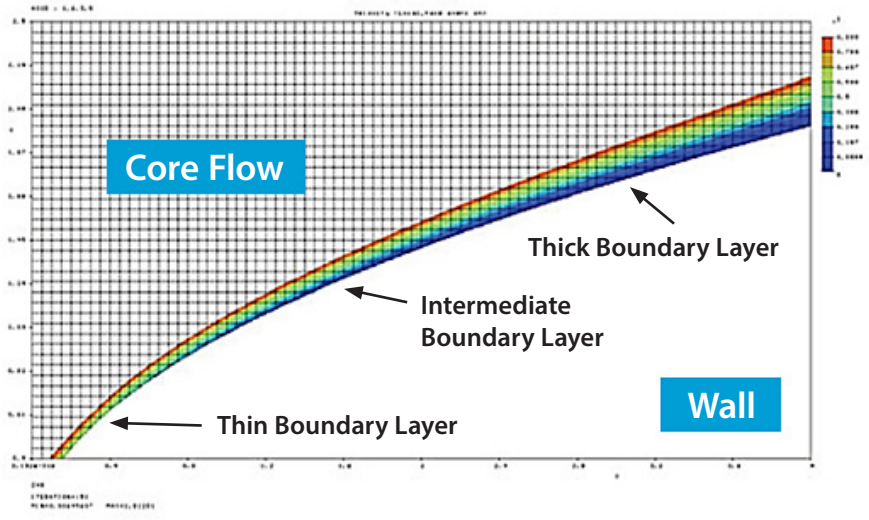

Figure 4: "Thin", "Intermediate" and "Thick" boundary layers.

Essentially such a turbulence modeling approach can be applied for dynamic as well as for temperature and concentrations boundary layers. In the thin-boundary-layer approach within FloTHERM XT, Prandtl boundary layer equations are used along fluid streamlines covering the walls (Ref 12). For their solution an integral boundary layer technology is applied (Ref 12). In the case of turbulent flows, for the determination of turbulent viscosity, the Van Driest hypothesis on the mixing length in turbulent boundary layers is used (Ref 13). The influence of wall roughness, considered as the equivalent sand grain roughness and the external flow's turbulence on the boundary layer are modeled through semi-empirical coefficients correcting the wall shear stress and the heat flux from the fluid to the wall. From a thin-boundary-layer calculation the boundary layer thickness, wall shear stress, and the heat flux from the fluid to the wall are calculated, and are used as boundary conditions for the Navier-Stokes equations. When the number of cells across a boundary layer is sufficient, a boundary layer modification of the well-known wall functions approach is used. However, instead of the classical approach where the logarithmic velocity profile is used, FloTHERM XT uses the full profile proposed by Van Driest (Ref 13). All other assumptions are similar to the classical wall functions approach in traditional CFD software.

The incorporation of a thin-boundary-layer approach is a key element of the FloTHERM XT SmartCells technique. Another similar engineering approach is used in the modeling of fluid flow phenomena in planar thin slots or cylindrical thin channels. Use of this technology in combination with a CAD/CFD bridge brings additional benefits for resolution of flows in dedicated elements of complex models where the number of mesh cells is not enough for full 3D modeling. Having direct access to the native CAD data, the FloTHERM XT technology platform can recognize that some geometry can form flow passages as pipes or thin channels, because this information exists in the CAD system. In such cases, analytical or empirical data is used to replace the 3D Navier-Stokes equations typically needed to model within such dedicated flow passages with minimal loss of accuracy. In addition to this resolution of fluid flow phenomena via effective simplified engineering approaches in SmartCells, the approach has also been applied successfully to heat transfer phenomena in solid thin walls and even over thin multilayer structures within one cell. Usage of other engineering methods also extends SmartCell models to various electronics devices such as PCBs, 2-Resistor Models, Heat Pipes, etc. with minimal grid cell counts. Extensive validations and verifications of FloTHERM XT's underlying technologies have been done by Ivanov et al (Ref 10).

INDUSTRIAL VALIDATIONS OF THE SMARTCELL TECHNOLOGY IN FloTHERM XT

PIN-FIN HEAT SINK

Free convection cooling performance of a pin-fin heatsink has been studied experimentally (Ref 14). The case of 9x9 square pin-fin array presented in this paper has been investigated via FloTHERM XT (Ref 15) and compared with the above measurements. The model exactly reproduces the experimental conditions. It consists of two rectangular Plexiglas enclosures, one inside another. The internal enclosure contains an aluminum pin-fin heatsink mounted on a heated component (see Figure 5).

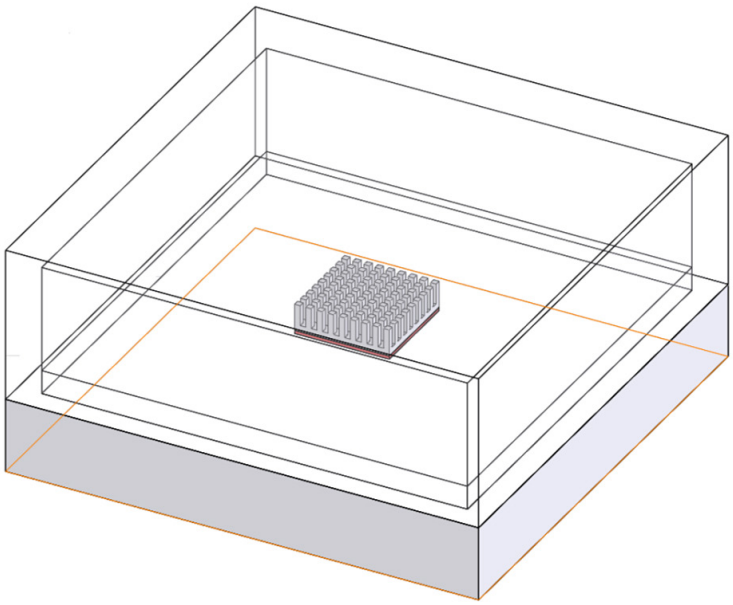

Figure 5: A close-up of the model: the internal enclosure with 9x9 pin-fin array over the heating component flush mounted on the bottom.

Two configurations are simulated. One with the heatsink mounted with the base horizontal, fins upward, and the other with the base vertical. Thermal conduction within the solid regions is modeled together with convection and radiative heat transfer.

Figure 6 shows a comparison of experimental visualization (image on right) with predicted flow pattern for heat generation rate Q = 1 W (central image) on a vertical plane through the center of the heatsink for the model with the base mounted vertically. The mesh, shown in the image on the left, consists of about 145,000 cells. The images show a high level of agreement between simulation and experiment.

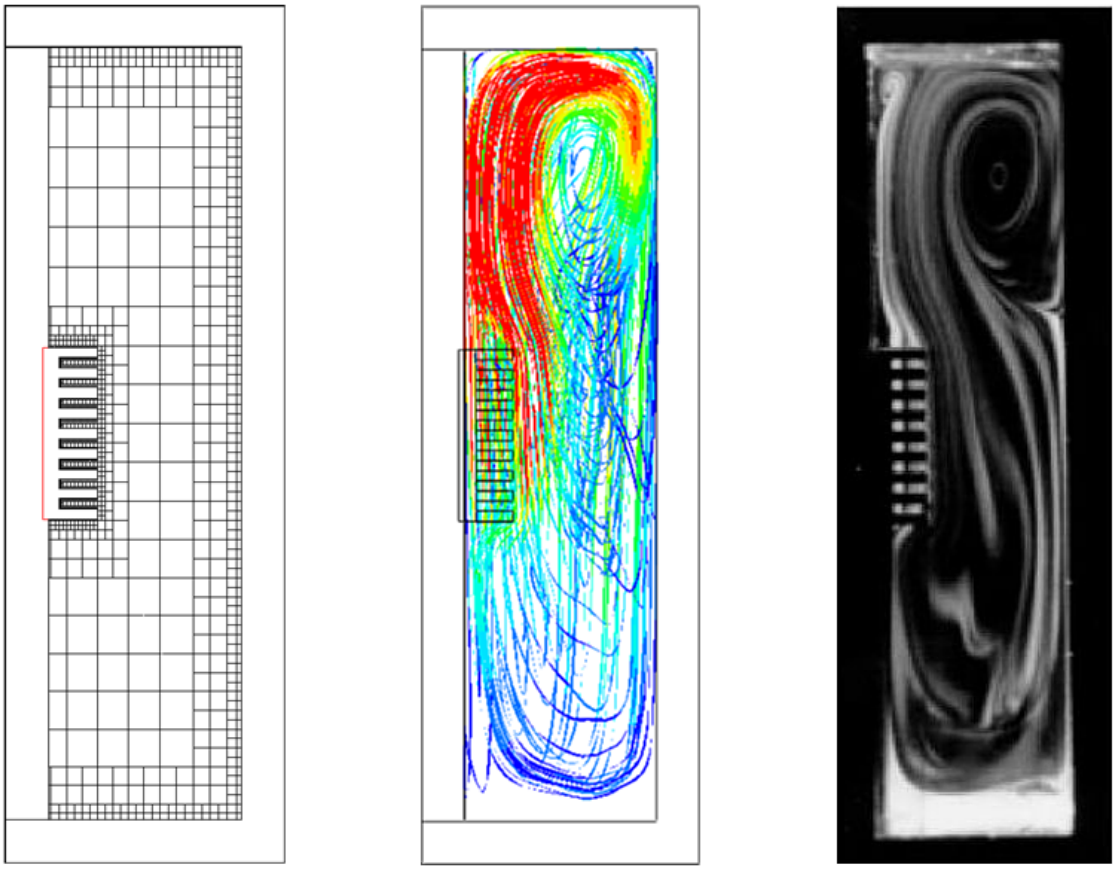

Figure 6: Mesh view (a), predicted flow trajectories colored by velocity magnitude (b) experimental visualization (c), Q = 1 W, vertical case, z = 0.

The next set of images show the comparison of the predicted flow pattern with experiment for the heatsink mounted horizontally. Figure 7, features a comparison of the experimental visualization (bottom image) with the predicted flow patterns for heat generation rate Q = 0.5 W (center image) on a vertical plane through the center of the heatsink. The mesh, shown in the top image, consists of about 142,000 cells.

A comparison of predicted and measured thermal resistance for considered cases shows that numerical results are within 5% of experimental data – an excellent correlation between computations and measurements. Note that the experimental results for the horizontal case are slightly non-symmetrical. This is due to the difficulty in maintaining uniform boundary conditions on the outer Plexiglas enclosure

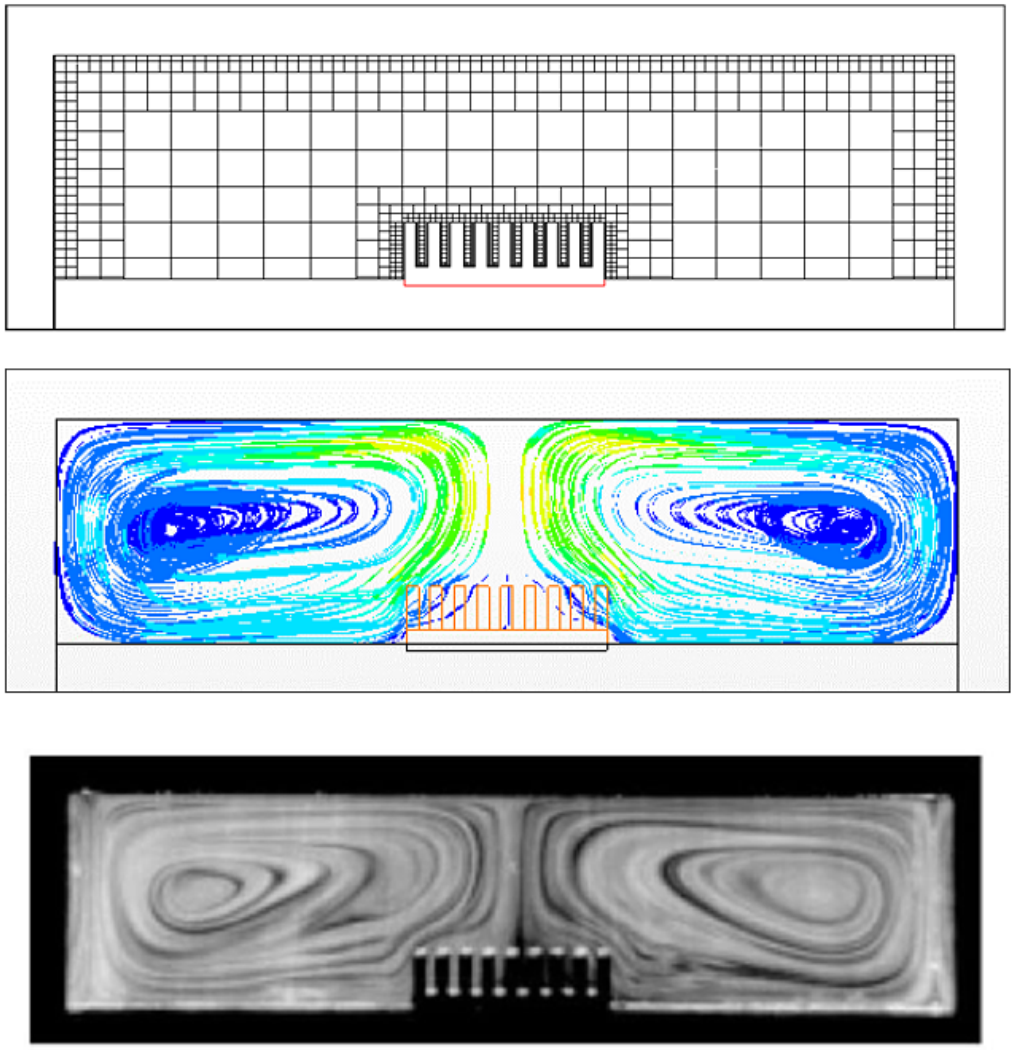

Figure 7: Visualization from [14], Q = 0.5 W, horizontal case, z = 0 m.

TRANSISTORS ON A WATER-COOLED COLD PLATE

This example follows the experimental investigation of transistors mounted on a cold plate (Ref 16). Consider a symmetrical array of transistors mounted on a cold plate as shown in Figure 8. The water-cooled cold plate supports sixteen 37.5 W stud-mounted transistors, modeled as a Network Assembly SmartPart, producing a total power dissipation of 600 W. The coolant flow rate is 62.8 g/s with an inlet temperature of 35°C, flowing through a 0.794 cm internal diameter tube. Silicone grease is used at the temperature mounting surface. It is necessary to determine the component surface temperature as the maximum allowable temperature is 71°C.

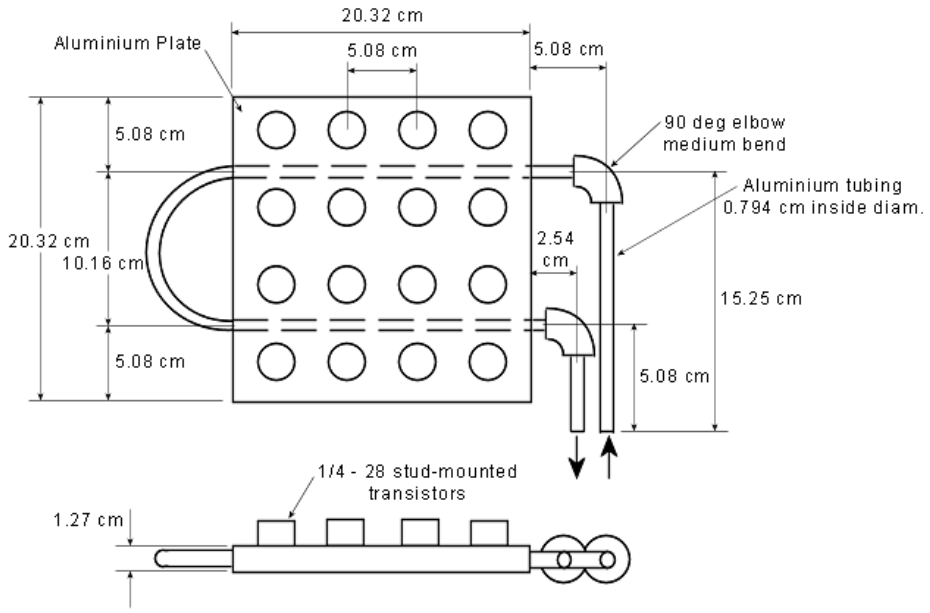

Figure 8: Transistor Array on a Cold Plate

The component surface temperature (in °C) can be calculated as:

$35 + \Delta t1 + \Delta t2 + \Delta t3 + \Delta t4$

Where:

$\Delta t1$ is the temperature rise across the transistor mounting interface from the transistor case to the heat sink surface, using silicone grease at the interface.

$\Delta t2$ is the temperature rise through the aluminum cold plate from the transistor to the coolant tubing.

$\Delta t3$ is the temperature rise across the liquid coolant convection film from the walls of the tube to the coolant.

$\Delta t4$ is the temperature rise of the coolant as it flows through the cold plate picking up heat from the transistors.

Figure 9 shows a cross section view of the model displaying the mesh in the cold plate fluid channel. A total of 46,000 mesh cells were used in this model.

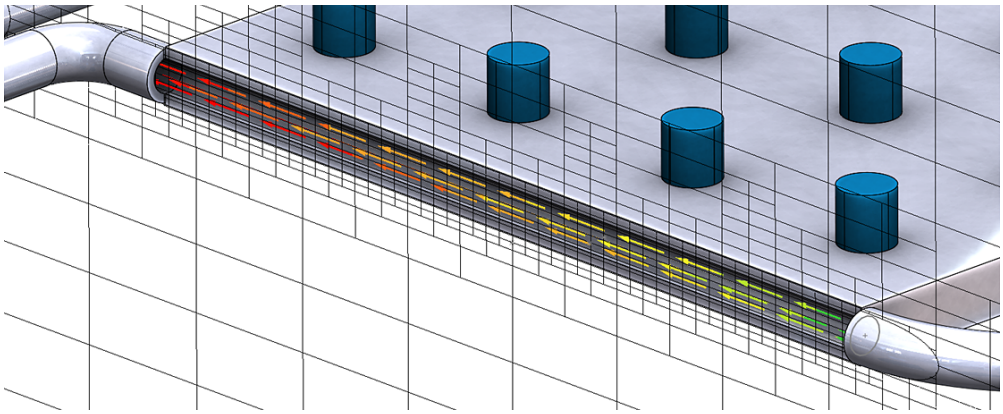

Figure 9: Cold Plate fluid channel mesh

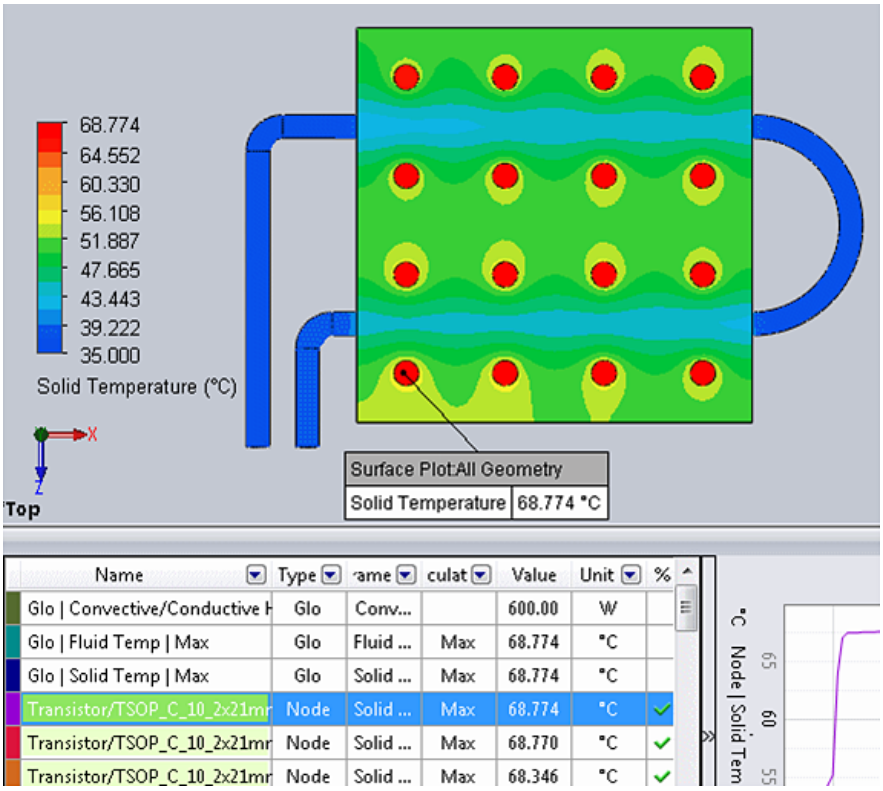

Figure 10: Surface Plot of FloTHERM XT Model

Figure 10 shows the temperature distribution on the transistor cold plate from FloTHERM XT. The calculated temperature rises used for comparison to the experimental results are shown in Table 2.

	Calculated Maximum Temperature (°C)	
	Theoretical	FloTHERM XT
Δt1	11.2	10.804
Δt2	11.5	12.315
Δt3	8.5	7.978
Δt4	2.3	2.287
Ambient	35	35
Total	**68.5**	**68.383**

Table 2: FloTHERM XT results comparison

FloTHERM XT matched the overall experimental temperature rise to within 0.35% with the worst temperature rise correlation at Δt2 with a difference of 7.1%. Overall the correlation between experiment and FloTHERM XT analysis is good. For a complete description of the analysis refer to the FloTHERM XT Validation Guide (Ref 17).

DETAILED INTEGRATED CIRCUIT PACKAGE

A detailed Integrated Circuit (IC) in a BGA208 package has been studied experimentally and analytically in FloTHERM XT (Ref 18). The IC package was mounted on JEDEC 2S2P and 2S0P (Figure 11) thermal test vehicles and powered in still-air and forced convection environments. A cross section of the IC package is shown in Figure 12 and Plan view in Figure 13.

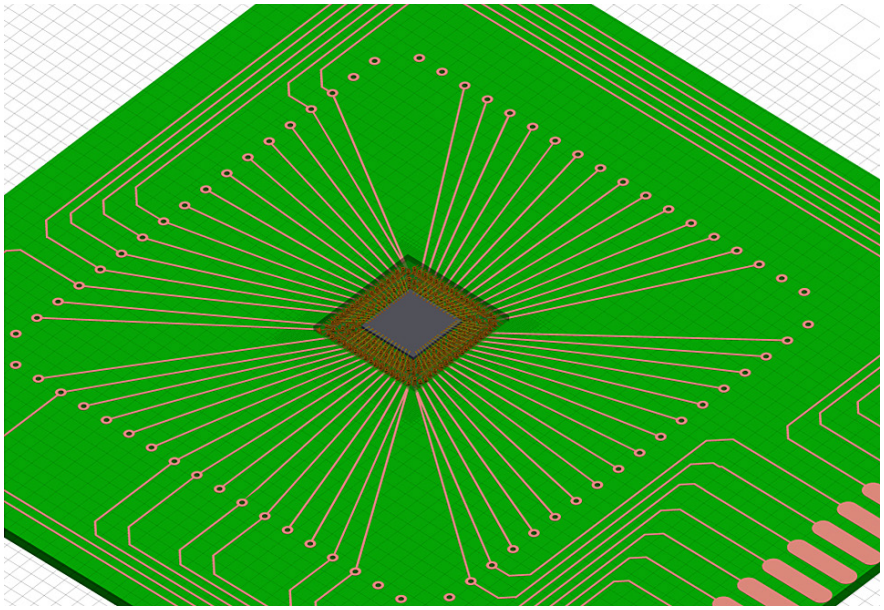

Figure 11: Detailed BGA208 mounted on 2S0P thermal test vehicle

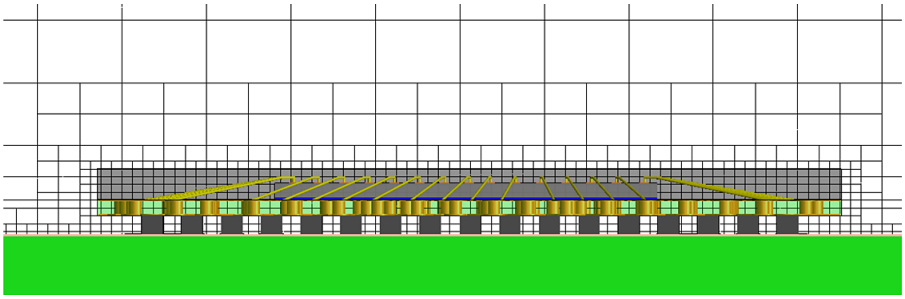

Figure 12: Detailed BGA208 Cross Section

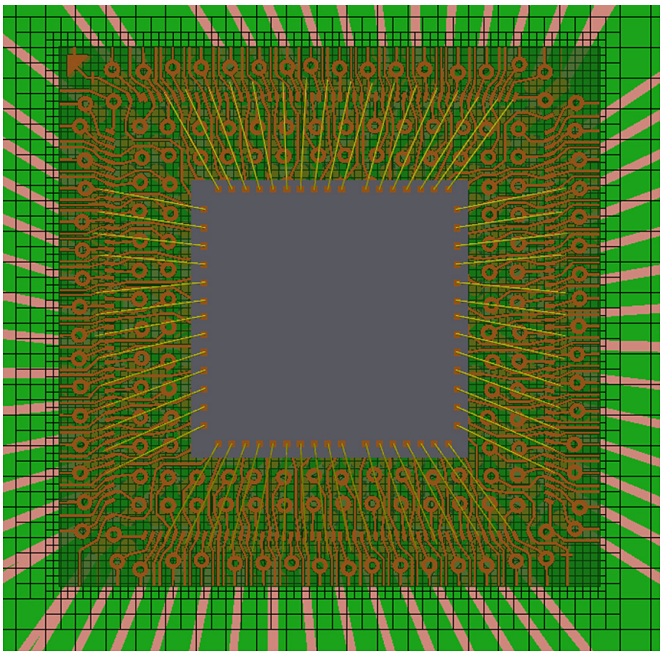

Figure 13: Detailed BGA208 Plan View

The focus of the study was to compare the results of the FloTHERM XT model with the experimental results with various modeling assumptions. Assumptions that were explored include:

- **Solder Ball resolution:** Spherical vs. Cuboidal
  - Cuboidal solder balls were modeled with the same cross sectional area
- **JEDEC thermal test vehicle trace resolution:** Discrete vs. Lumped
  - Lumped thermal test vehicle thermal conductivities
    - 1S0P: $k_x = k_y = 2.54$W/mK, $k_z = 0.405$W/mK
    - 2S2P: $k_x = k_y = 19.37$W/mK, $k_z = 0.424$W/mK
- **Bond Wires:** With and Without

The sensitivity study showed that the solder ball modeling resolution accounted for a junction temperature difference of less than 0.5%. The lumped approximation to the thermal test vehicle resulted in significant error in the junction temperature prediction, particularly with the 2S0P board, as shown in Table 3.

	V [m/s]		
	1	2	3
2S0P	12	16	16
2S2P	2.1	2.5	3.5

Table 3: Lumped Thermal Test Vehicle %Error

Including the bond wires in the analysis lowered the junction temperature by 3°C, accounting for 4% error when not including them.

When considering the cuboidal solder ball representation, detailed thermal test vehicles, and bond wires there was excellent agreement between the FloTHERM XT model (Figure 14) and experimental results. The Junction temperature prediction of the detailed FloTHERM XT model agreed to within 2% of the experimental results.

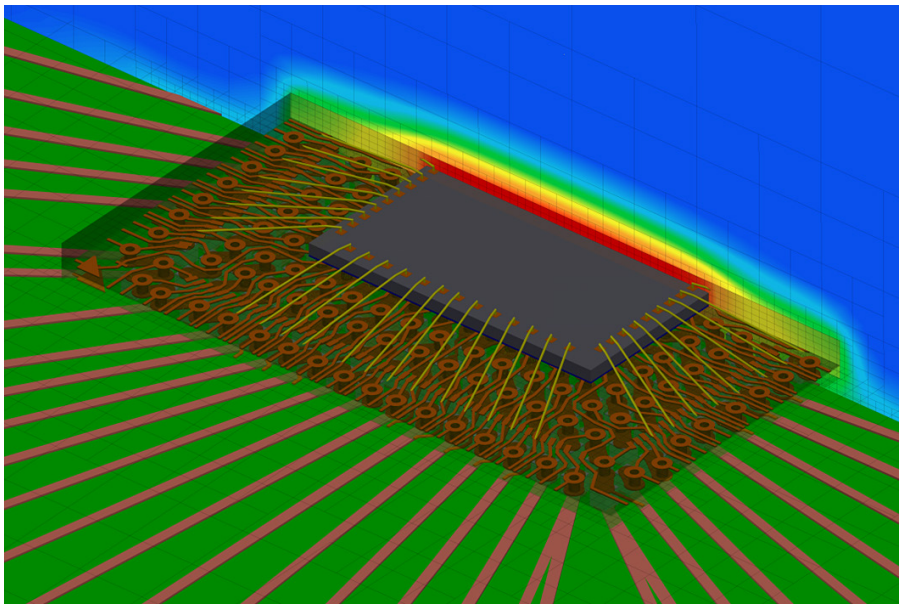

Figure 14: 2S0P Detailed BGA208, V=3 m/s

CONCLUSION

The biggest barrier to user productivity with industrial CFD tools today is dealing quickly and effectively with complex CAD geometries by generating usable meshes within realistic engineering timescales. Efficient usage of CAD-centric CFD tools (like FloTHERM XT) requires the development of special engineering models that allow for rapid, robust and accurate solutions. Such approaches can be realized by the usage of a technology based on the synergy of numerical and engineering methods applied to solutions of fluid dynamics and heat transfer tasks on rectangular adaptive grids - the SmartCells technique. FloTHERM XT, based on this technology, produces high levels of accuracy in an efficient, practical tool for both thermal experts and mechanical engineers, to solve large, complex electronic systems. SmartCells can mesh complex geometries in seconds and minutes versus, hours, days and even weeks for traditional CFD meshing approaches. The approach can be applied to different stages of manufacturing design cycles and it allows for the optimal situation of frontloading of simulation technologies in order to keep up with global product manufacturing competition. It also solves the age-old "Achilles heel" of CFD, the time-consuming specialist nature of mesh generation, thus paving the way for the democratization of CFD usage.

REFERENCES

1. Sobachkin A.A., Dumnov G.E. Numerical Basis of CAD-Embedded CFD. Proceedings of NAFEMS World Congress NAFEMS World Congress, Austria, Salzburg, June, 2013.
2. Hanna, R. K., Parry, J., "Back to the Future: Trends in Commercial CFD", NAFEMS World Congress, Boston, USA, June, 2011
3. Boysan, H.F., Choudhury, D. & Engelman, M.S., "Commercial CFD in the Service of Industry: The First 25 Years" in 'Notes on Numerical Fluid Mechanics and Multidisciplinary Design', Volume 100, 2009, pp. 451-461
4. Spalding, D. B., "CFD Past, Present and the Future", Lecture at the Sixteenth Leont'ev School-Seminar Saint Petersburg, Russia, May 21-25, 2007, http://www.cham.co.uk/Docs/CFDeng3.ppt
5. Launder, B.E.; Spalding, D.B., "The numerical computation of turbulent flows". Computer Methods in Applied Mechanics and Engineering. 3 (2): 269–289, March 1974. doi:10.1016/0045-7825(74)90029-2
6. Marovic Boris. "The New Role of CFD in the Ever Faster Development Cycle and the Struggle with Complex Geometries of the Lighting Industry." ISAL 2013 (Darmstadt, Germany), Sept. 2013.
7. Dumnov, G., Kharitonovich, A., Marovic, B.; and Sobachkin A., "Simulation Time Saving Approach Based on the Synergy of Numerical and Engineering Methods for Experts and Design Engineers", FISITA Automotive Congress, September 2016, Busan, South Korea.
8. Sabeur, M., "Frontloading CFD in the Automotive Development Process", NAFEMS European Conference, December 2015, Munich, Germany.
9. Weinhold, I., Parry, J., "The Third Wave of CFD", NAFEMS World Congress, Austria, Salzburg, June, 2013.
10. Ivanov A.V., Trebunskikh T.V., Platonovich V.V. "Validation Methodology for Modern CAD-Embedded CFD Code: From Fundamental Tests to Industrial Benchmarks." Proceedings of NAFEMS World Congress NWC 2013, Austria, Salzburg, June 09-12, 2013.
11. Uppuluri Sudhindra, Proulx Joe, Marovic Boris, Naiknaware Ajay. "Characterizing Thermal Interactions between Engine Coolant, Oil and Ambient for an Internal Combustion Engine." SAE World Congress 2013 (Detroit, MI, USA), April 2013.
12. Lam C.K.G., Bremhorst K.A. "Modified Form of Model for Predicting Wall Turbulence." ASME Journal of Fluid Engineering, 1981, 103: 456-460.
13. Van Driest E.R. "On Turbulent Flow near a Wall." Journal of the Aeronautical Science, 1956, 23(10): 1007.

14. Yu, E. and Joshi, Y., 2002. Heat Transfer Enhancement from Enclosed Discrete Components Using Pin-Fin Heat Sinks. Int. J. Heat Mass Transfer, Vol. 45, No. 25, pp 4957-4966.

15. Balakin, V. Churbanov, A. Gavriliouk, V. Makarov, M. and Pavlov, A., 2004. Verification and Validation of EFD.Lab Code for Predicting Heat And Fluid Flow, Proceedings of CHT-04 ICHMT International Symposium on Advances in Computational Heat Transfer, April 19-24, Norway, CHT-04-179

16. Steinberg, Dave S., 1991, Cooling Techniques for Electronic Equipment, Second Edition

17. Mentor Graphics Corp., 2011, FloTHERM XT Validation Reference Guide

18. Bissuel, Daniel, and Monier-Vinard, 2015, Thales, Numerical and Experimental Thermal Study of a Detailed BGA Model with FloTHERM

For the latest product information, call us or visit: www.mentor.com

Corporate Headquarters
Mentor Graphics Corporation
8005 SW Boeckman Road
Wilsonville, OR 97070-7777
Phone: 503.685.7000
Fax: 503.685.1204

Sales and Product Information
Phone: 800.547.3000
sales_info@mentor.com

Visit www.mentor.com/company/office_locations/ for the list of Mechanical Analysis Division Offices

MGC 01-17 TECH15150